Inherited chromosomally integrated human herpesvirus 6 genomes are ancient, intact and potentially able to reactivate from telomeres

Inherited chromosomally integrated human herpesvirus 6 genomes are ancient, intact and potentially able to reactivate from telomeres

Enjie Zhang [a], Adam J Bell [b], Gavin S Wilkie [b], Nicolás M Suárez [b], Chiara Batini [c], Colin D Veal [a], Isaac Armendáriz-Castillo [a], Rita Neumann [a], Victoria E Cotton [a], Yan Huang [a], David J Porteous [d], Ruth F Jarrett [b], Andrew J Davison [b], Nicola J Royle [a] #

[a] Department of Genetics, University of Leicester, Leicester, UK

[b] MRC-University of Glasgow Centre for Virus Research, Glasgow, UK

[c] Department of Health Sciences, University of Leicester, Leicester, UK

[d] Generation Scotland, Centre for Genomic and Experimental Medicine, Institute of Genetics and Molecular Medicine, University of Edinburgh, UK

Address correspondence to Nicola J. Royle, njr@le.ac.uk

Tel: +44 (0)116-2522270

Key words: Human herpesvirus 6, telomere, integration, ciHHV-6, molecular dating, Generation Scotland

Short title: Ancient ciHHV-6 genomes maybe capable of reactivation

ABSTRACT

The genomes of human herpesviruses 6A and 6B (HHV-6A and HHV-6B) have the capacity to integrate into telomeres, the essential capping structures of chromosomes that play roles in cancer and ageing. About 1% of people worldwide are carriers of chromosomally integrated HHV-6 (ciHHV-6), which is inherited as a genetic trait. Understanding the consequences of integration for the evolution of the viral genome, for the telomere and for the risk of disease associated with carrier status is hampered by a lack of knowledge about ciHHV-6 genomes. Here, we report an analysis of 28 ciHHV-6 genomes and show that they are significantly divergent from the few modern non-integrated HHV-6 strains for which complete sequences are currently available. In addition ciHHV-6B genomes in Europeans are more closely related to each other than to ciHHV-6B genomes from China and Pakistan, suggesting regional variation of the trait. Remarkably, at least one group of European ciHHV-6B carriers has inherited the same ciHHV-6B genome, integrated in the same telomere allele, from a common ancestor estimated to have existed 24,500 ±10,600 years ago. Despite the antiquity of some, and possibly most, germline HHV-6 integrations, the majority of ciHHV-6B (95%) and ciHHV-6A (72%) genomes contain a full set of intact viral genes and therefore appear to have the capacity for viral gene expression and full reactivation.

IMPORTANCE

Inheritance of HHV-6A or HHV-6B integrated into a telomere occurs at a low frequency in most populations studied to date but its characteristics are poorly understood. However, stratification of ciHHV-6 carriers in modern populations due to common ancestry is an important consideration for genome-wide association studies that aim to identify disease risks for these people. Here we present full sequence analysis of 28 ciHHV-6 genomes and show

47 that ciHHV-6B in many carriers with European ancestry most likely originated from ancient
48 integration events in a small number of ancestors. We propose that ancient ancestral origins
49 for ciHHV-6A and ciHHV-6B are also likely in other populations. Moreover, despite their
50 antiquity, all of the ciHHV-6 genomes appear to retain the capacity to express viral genes, and
51 most are predicted to be capable of full viral reactivation. These discoveries represent
52 potentially important considerations in immune-compromised patients, in particular in organ
53 transplantation and in stem cell therapy.

54

INTRODUCTION

Given the complex roles that human telomeres play in cancer initiation and progression and in ageing (1, 2), it is remarkable that the genomes of human herpesviruses 6A and 6B (HHV6-A and HHV-6B; species *Human betaherpesvirus 6A* and *Human betaherpesvirus 6B*) can integrate and persist within them (3). Human telomeres comprise double-stranded DNA primarily composed of variable lengths of $(TTAGGG)_n$ repeats and terminated by a 50-300 nucleotide (nt) 3' single-strand extension of the G-rich strand. Telomeres, bound to a six-protein complex called shelterin, cap the ends of chromosomes and prevent inappropriate double-strand break repair. They also provide a solution to the 'end replication problem' via the enzyme telomerase (4-6).

The double-stranded DNA genomes of HHV-6A and HHV-6B consist of a long unique region (U; 143-145 kb) encoding many functional open reading frames (ORFs U2-U100), flanked by identical left and right direct repeats (DR_L and DR_R; 8-10 kb) encoding two ORFs (DR1 and DR6). Each DR also contains near its ends two variable regions of telomere-like repeat arrays (T1 and T2) (7, 8), terminated by the viral genome packaging sequences (PAC1 and PAC2, respectively) (9, 10). Telomeric integration by HHV-6A or HHV-6B (yielding chromosomally integrated HHV-6, ciHHV-6) results in loss of the terminal PAC2 sequence at the fusion point between the telomere and DR_R-T2 (11) and loss of the DR_L-PAC1 sequence at the other end of the integrated viral genome when the DR_L-T1 degenerate telomere-like repeat region becomes part of a newly formed telomere (Figure 1A, (12)).

Once the HHV-6 genome has integrated in the germline it can be passed from parent to child, behaving essentially as a Mendelian trait (inherited ciHHV-6) (13-16). The telomere carrying the ciHHV-6 genome shows instability in somatic cells, which can result in the

partial or complete release of the viral genome as circular DNA (12, 17, 18). This could represent the first step towards viral reactivation, and in this respect telomeric integration may be a form of HHV-6 latency. To date, reactivation of ciHHV-6 has been demonstrated *in vivo* in two settings: first, in a child with X-linked severe combined immunodeficiency who was also a carrier of inherited ciHHV-6A (19); and second, upon transplacental transmission from two ciHHV-6 carrier mothers to their non-carrier babies (20). Recently, it has been shown that ciHHV-6 carriers bear an increased risk of angina pectoris (21), although it is not known whether this arises from viral reactivation, a deleterious effect on the telomere carrying the viral genome, or some other mechanism.

A small proportion of people worldwide are carriers of inherited ciHHV-6A or -6B, but very little is known about the HHV-6 genomes that they harbor, although this may influence any associated disease risk. To investigate ciHHV-6 genomic diversity and evolution, the frequency of independent germline integrations, and the potential functionality of the integrated viral genomes, we analysed 28 ciHHV-6 genomes. We discovered that ciHHV-6 genomes are more similar to one another than to the few sequenced reference HHV-6 genomes from non-integrated viruses. This is particularly marked among the ciHHV-6B genomes from Europeans. We also found that a subset of ciHHV-6B carriers from England, Orkney and Sardinia are most likely descendents from a single ancient ancestor. Despite the apparent antiquity of some, possibly most, ciHHV-6 genomes, we concluded that the majority contain a full set of intact HHV-6 genes and therefore in principle retain the capacity to generate viable viruses.

MATERIAL AND METHODS

Population screening to identify ciHHV-6 carriers. ciHHV-6 carriers were identified by screening a variety of DNA sample collections of individuals from across the world, using

PCR assays to detect either U11, U18, DR5 (HHV-6A) or DR7 (HHV-6B) (12), or U7, DR1, DR6A or DR6B ((22) and manuscript in preparation). DR5, DR6A, DR6B and DR7 correspond to ORFs in the original annotation of the HHV-6A genome (GenBank accession X83413 (23)), but DR5 is in a non-coding region of the genome, and DR6A, DR6B and DR7 are in exons of DR6 in the reannotation used (RefSeq accession NC_001664). From the populations screened, 58 samples with ciHHV-6 among 3875 individuals were identified (Table 1). The number of individuals screened in most populations was small and therefore cannot be used to give an accurate estimate of ciHHV-6A or -B frequencies, although a larger number of ciHHV-6B-positive samples was identified overall. The frequency of ciHHV-6B carriers in Orkney (1.9%), a collection of islands off the north coast of Scotland, is higher than that reported from England (24). Screening of the Generation Scotland: Scottish Family Health Study (GS:SFHS) will be described elsewhere (RFJ, manuscript in preparation). Ethical approval for the GS:SFHS cohort was obtained from the Tayside Committee on Medical Research Ethics (on behalf of the National Health Service).

Generation of overlapping amplicons and sequencing. The 32 primer pairs used to generate overlapping amplicons from ciHHV-6A genomes, and the PCR conditions employed, were reported previously (18). The primer pairs used to amplify ciHHV-6B genomes were based on conserved sequences from the HHV-6B non-integrated HST and Z29 strains (Genbank accessions AB021506.1 and AF157706 respectively; (9, 25). The primer sequences are shown in Supplementary Table S1. The amplicons from each sample were pooled in equimolar proportions and then sequenced by using the Illumina MiSeq or IonTorrent (Life Technologies) next-generation sequencing platforms, as described previously (18). Some sequences were verified by using Sanger dideoxy chain termination sequencing on PCR-amplified products.

Assembly and analysis of DNA sequence data. DNA sequence data were processed essentially as described previously (18), except that SPAdes v. 3.5.0 (26) was used for *de novo* assembly into contigs, ABACAS v. 1.3.1 (27) was used to order contigs, and Gapfiller v. 1-11 (28) was used to fill gaps between contigs. The integrity of the sequences was verified by aligning them against the read data using BWA v. 0.6.2-r126 and visualizing the alignments as BAM files using Tablet v. 1.13.08.05. Nucleotide substitutions, indels and repeat regions were also verified by manual analysis using IGV v. 2.3 (http://software.broadinstitute.org/software/igv/home).

Alignments of the seven ciHHV-6A genomes with the three published HHV-6A genomes from non-integrated strains U1102, GS and AJ (23, 29-31), and alignment of the 21 ciHHV-6B genomes with the two previously published HHV-6B genomes from non-integrated viruses HST and Z29 (9, 25), were carried out by using Gap4 (32). Variation across the ciHHV-6 genomes was studied by a combination of manual inspection and automated analysis by using an in-house Perl script. The script performed a sliding window count of substitutions using the aligned Gap4 files, reporting the count according to the mid-point of the window. For analysis across the genome, the window size was 1 kb and the step size was 1 nucleotide. For analysis of individual ORFs, a file with a list of annotated positions was generated.

Phylogenetic analyses were carried out by using two different methods. Maximum likelihood trees were built by using the maximum composite likelihood model (MEGA6.0), and bootstrap values were obtained with 2000 replications. Model selection was carried out for HHV-6A and HHV-6B separately, and the substitution model with the lowest Bayesian information criterion was selected (the Tamura 3-parameter model (33) for HHV-6B and the Hasegawa-Kishino-Yano model for HHV-6A). Median-joining networks were built by using Network 5.0 (www.fluxus-engineering.com) with default parameters. Sites with missing data

were excluded from all phylogenetic analyses for both HHV-6A and HHV-6B. The number of positions analysed for HHV-6B was 130412, and that for HHV-6A was 117900. The time to the most recent common ancestor (TMRCA) was calculated by using rho as implemented in Network 5.0. Rho values were transformed into time values by using the accepted mutation rate for the human genome, 0.5E-09 substitutions per bp per year (34), scaled to the number of sites analysed.

Comparison of tandem repeat regions. The copy numbers of repeat units in the DR-R, R0, R1, R2, R3 and R4 tandem repeat regions (9, 25) were determined by manual inspection of the individual BAM files generated for each sequenced ciHHV-6 genome, with verification by checking the sequence alignments generated using Gap4. The numbers of copies of TTAGGG in each DR_L-T2 region was determined from PCR amplicons generated using the DR8F and UDL6R primers (Supplementary Table S1). Each amplicon was purified using a Zymoclean™ gel DNA recovery kit, and then sequenced by using the Sanger dideoxy chain termination method. The sequence data were analysed by using the MacVector software. Variation at the $(CA)_n$ repeat array located immediately adjacent to T1 in HHV-6B was investigated in DR_L specifically by reamplification of single telomere length analysis (STELA (35)) products, using the primers DR1R and TJ1F. The short amplicons were purified and sequenced as above and compared with the same sequence in the reference HST and Z29 genomes.

Analysis of DR_R-T1 region by TVR-PCR

The DR_R-T1 regions from ciHHV-6B positive samples were amplified by using the primers U100Fw2 and DR1R. Telomere variant repeat mapping by PCR (TVR-PCR) was conducted on each of these amplicons essentially as described before (36, 37) but using an end-labeled primer, HHV-6B-UDR5F and the unlabeled TAG-TELWRev. The TELWRev primer anneals

176 to TTAGGG repeats, allowing amplification of products that differ in length depending on the
177 location of the TTAGGG repeat with respect to the flanking primer (HHV-6B-UDR5F). The
178 labeled amplicons from the T1 region were separated by size in a 6% denaturing
179 polyacrylamide gel.

180 **Analysis of HHV-6 ORFs.** The frequency of nucleotide substitutions in each ORF was
181 determined by a combination of manual inspection and automated analysis using a Perl script,
182 as described above. The DNA sequences of each of the 86 HHV-6B ORFs from the 21
183 ciHHV-6B genomes were aligned to identify and compare the number of synonymous and
184 non-synonymous codon changes within and among genes. In addition the predicted amino
185 acid sequences for each gene in the 21 ciHHV-6B genomes were aligned to confirm the
186 number of non-synonymous changes.

187 **Characterisation of chromosome-ciHHV-6 junctions.** The junctions between the
188 chromosome and the ciHHV-6 genome were isolated by PCR amplification using various
189 primers that anneal to subterminal regions of a variety of human chromosomes in
190 combination with the DR8F primer. The amplicons were purified as described above and
191 sequenced by using the Sanger method with a variety of primers (Supplementary Table S1).
192 The number of repeats present in each junction fragment and the interspersion of TTAGGG
193 repeats with degenerate repeats was determined by manual inspection using the MacVector
194 software.

195 **Accession numbers.**

196 The finished sequences have been deposited in GenBank under accession numbers
197 KY316030-KY316056 (Table 2). The LEI_1501 ciHHV-6A genome reported previously has
198 the accession number KT355575 (doi: 10.1038/srep22730)(18).

199

RESULTS

Selection of ciHHV-6 carriers and sequence analysis of viral genomes. To investigate sequence variation among ciHHV-6 genomes, 28 samples were selected for analysis: seven with ciHHV-6A (including LEI-1501 (18)) and 21 with ciHHV-6B (Table 2). The selected samples were identified in the various populations screened (Table 1), and included additional individuals from the London area (16), Scotland and the north of England (22), the Leicester area of England (18) and the GS:SFHS (RJF, manuscript in preparation). The chromosomal location of ciHHV-6 genomes, determined by fluorescent *in situ* hybridisation (FISH), was available for some samples (16, 18). For other samples the junction between the viral DR8 sequence (a non-coding region near one end of DR) and the chromosome subtelomeric region was isolated by PCR and sequenced (discussed below). Integration of each ciHHV-6 genome was confirmed by detection of a telomere at DR_L-T1 using STELA (12), or by detection of at least one copy per cell using droplet digital PCR (22, 38).

Each viral genome from ciHHV-6 carriers was sequenced from pooled PCR amplicons (12, 18). Full sets of HHV-6 amplicons were readily generated (Fig. 1 and Supplementary Table S1), demonstrating the robustness of this approach for enriching HHV-6 sequences from ciHHV-6 carriers. The HHV-6 amplicons generated from each carrier had the expected sizes, with variation only in amplicons encompassing repetitive regions (e.g. the DR_R-T1 region of degenerate telomere-like repeats). This observation indicated that all of the ciHHV-6 genomes are essentially intact, with the exception of the terminal DR_R-PAC2 and DR_L-PAC1 sequences lost during integration (Fig. 1A) (11, 12).

The ciHHV-6 genome sequences were determined by short-read next-generation sequencing (NGS), with some verification by the Sanger method. *De novo* assemblies of each genome were generated with few gaps (Fig. 1*).* The finished sequences were annotated and

224 deposited in GenBank under accession numbers KY316030-KY316056 (Table 2). The
225 ciHHV-6A genome reported previously by us was included in these analyses *(*LEI-1501,
226 KT355575; (18)).

227 **Sequence similarity is greater among ciHHV-6 genomes than to non-integrated HHV-6**
228 **genomes.** Nucleotide substitution frequencies were analysed across the DR and U regions of
229 the HHV-6B genome (excluding the tandem repeat regions R-DR, R0, R1, R2, R3 and R4,
230 see Fig. 1, (9, 25)) for each sequenced ciHHV-6B genome in comparison with the two
231 available HHV-6B reference genomes from non-integrated strains (HST from Japan,
232 GenBank accession AB021506, (25) and Z29 from Democratic Republic of Congo
233 (D.R.Congo), GenBank accession AF157706, (9)). The ciHHV-6B genomes show different
234 patterns of variation from the reference genomes, with greater divergence from strain Z29 in
235 the distal portion of the U region (120-150 kb) and across DR (1-8 kb), reaching a maximum
236 of 35 substitutions per kb in these regions (Fig. 2A). Overall, there is less divergence from
237 strain HST, although the frequency of substitutions is higher in part of the U region (45-64
238 kb) compared to strain Z29. To assess sequence variation among the ciHHV-6B genomes,
239 comparisons were made using the genome in HAPMAP NA10863 (CEPH1375.02) as a
240 reference. The substitution frequency is considerably less across the viral genomes for 18/20
241 of the ciHHV-6B genomes from individuals with European ancestry, indicating greater
242 similarity among them. Notably, the other two ciHHV-6B genomes that showed a higher
243 substitution frequency in this comparison were in individuals from Pakistan and China,
244 HGDP00092 and HGDP00813, respectively (Fig. 2A).

245 Nucleotide substitution frequencies were also analysed across each of the seven
246 ciHHV-6A genomes in comparison with three non-integrated HHV-6A reference genomes
247 (strain U1102 from Uganda (39) (accession X83413, (23)); strain GS from the USA
248 (accessions KC465951.1 (GS1) and KJ123690.1 (GS2) (29, 30)) and strain AJ from the

Gambia (accession KP257584.1 (31)). This analysis shows that the ciHHV-6A genomes have similar levels of divergence from each reference genome from non-integrated HHV-6A and that divergence is highest across DR and the distal part of U (120-149 kb) (Fig. 2B). Comparisons with the ciHHV-6A LEI-1501 genome (18) as a reference, also showed greater similarity among the ciHHV-6A genomes although the substitution frequencies are higher than among European ciHHV-6B genomes, indicating greater diversity among the ciHHV-6A genomes sequenced here (40). Notably the ciHHV-6A in the Japanese individual (HAPMAP NA18999) shows greater divergence from the other ciHHV-6A samples of European origin.

In summary, comparisons of nucleotide substitution frequencies show that the viral genomes in ciHHV-6B carriers are more similar to each other than they are to reference genomes derived from clinical isolates of non-integrated HHV-6B from Japan (HST) and D.R.Congo (Z29). The ciHHV-6A genomes are also more similar to each other than they are to the three HHV-6A reference genomes, although this is less pronounced than among the ciHHV-6B genomes.

Phylogenetic analysis of ciHHV-6 and non-integrated HHV-6 genomes. Consistent with the results shown in Fig. 2, phylogenetic analysis of the U region from 21 ciHHV-6B and the HST and Z29 reference genomes (excluding DR, the large repeat regions and missing data shown in Fig. 1) shows that the ciHHV-6B genomes in HGDP00813 from China and HGDP00092 from Pakistan are outliers to the 19 ciHHV-6B genomes from individuals of European descent (Fig. 3A). A phylogenetic network of the ciHHV-6B genomes with European ancestry shows three clusters of 8, 3 and 5 closely related ciHHV-6B genomes (groups 1, 2 and 3, respectively; Fig. 3B) and three singletons (ORCA1340, COR264 and 1-ciHHV-6B). Phylogenetic analysis of DR alone shows that, with the exception of COR264, the European ciHHV-6B samples show greater similarity to the HST (Japan) reference genome than to the Z29 (D.R.Congo) reference genome. However, the DRs in the two non-

European ciHHV-6B samples HGDP000813 (China) and HGDP00092 (Pakistan) do not cluster closely with those in the European ciHHV-6B samples again indicating these ciHHV-6B strains are distinct (Supplementary Fig. S1 and Fig. 3A).

To explore variation only within HHV-6B genes, the frequency of substitutions in ORFs of each of the 21 ciHHV-6B genomes was compared with that in the HST and Z29 reference genomes and the ciHHV-6B genome in HAPMAP NA10863 (Fig. 4A). The patterns of variation were similar to those observed across the whole genome (Fig. 2A) and consistent with the phylogenetic analysis showing greater similarity among ciHHV-6B in Europeans and with the subgroups. Phylogenetic analysis of specific genes, which were selected because they show greater sequence variation from the reference genomes or among the ciHHV-6B genomes, generated a variety of trees that are generally consistent with the phylogenetic analysis based on the U region but exhibited less discrimination between samples or groups (Fig. 4 and Supplementary Fig. S2). For example, the phylogenetic tree based on U90 separates the European ciHHV-6B samples from the ciHHV-6B samples from China and Pakistan and from the HST and Z29 reference genomes but does not subdivide the European ciHHV-6B samples.

Phylogenetic analysis of the seven ciHHV-6A genomes and four reference genomes (U1102 (Uganda), AJ (Gambia) and two sequences from GS (USA)) shows a clear separation between the integrated and non-integrated genomes (Fig. 3C and D), with two pairs of closely related ciHHV-6A genomes (LEI-1501 and GLA_25506; 7A-17p13.3 and GLA_15137). A similar separation of the integrated versus non-integrated genomes is also evident in the phylogenetic analysis of DR alone, irrespective of the geographic origin of the individual ciHHV-6A carrier (Supplementary Fig. S1).

297 Variation within HHV-6A genes was also explored by plotting base substitution
298 frequency per ORF for each of the seven ciHHV-6A samples in comparison to the three
299 reference genomes and the ciHHV-6A genome in LEI_1501 (Fig. 4B). The patterns of
300 variation are similar to those observed across the whole genome (Fig. 2B). Phylogenetic
301 analysis of U83, U90 and DR6, selected because they show greater sequence variation,
302 generally support the phylogenetic trees and networks generated from analysis of the U and
303 DR regions (Supplementary Fig. S3).

304 Overall, the sequence variation and phylogenetic analyses indicate a divergence
305 between the integrated and non-integrated HHV-6 genomes but with some differences
306 between the HHV-6A and HHV-6B. The ciHHV-6B samples from individuals with European
307 ancestry showed divergence from both HST (Japan) and Z29 (D.R.Congo) reference
308 genomes, although the pattern of divergence varies across the genome. The 21 ciHHV-6B
309 genomes from individuals with European ancestry are more similar to one another than to the
310 ciHHV-6B genomes from China and Pakistan and can be subdivided into distinct groups.
311 There is greater divergence among the seven ciHHV-6A genomes than among the ciHHV-6B
312 genomes but, despite this, two pairs of closely related ciHHV-6A genomes were identified.

313 From these analyses, we concluded that the three groups of closely related ciHHV-6B
314 genomes and the pairs of ciHHV-6A genomes identified in the phylogenetic networks (Fig.
315 3B and D, respectively) could represent independent integrations by closely related strains of
316 HHV-6B or HHV-6A. Alternatively, each group might have arisen from a single integration
317 event, with members sharing a common ancestor. Further analyses were undertaken to
318 explore these possibilities.

319 **Comparison of tandem repeat regions in ciHHV-6 genomes.** Tandem repeat arrays within
320 the human genome often show length variation as a consequence of changes to the number of

repeat units present (copy number variation). The greater allelic diversity in these regions reflects the underlying replication-dependent mutation processes in tandem repeat arrays, which occur at a higher rate than base substitutions (41). To explore diversity among the ciHHV-6B genomes further, tandem repeat regions distributed across the viral genome were investigated. The R-DR, R2A, R2B and R4 repeat regions analysed (location shown in Fig. 1C) showed little or no copy number variation among the ciHHV-6B and non-integrated reference genomes (Fig. 5A, Table 3). Copy number variation at R1 (location shown in Fig. 1C) was greater but did not show a clear relationship with strains of ciHHV-6B or non-integrated HHV-6B. Greater copy number variation was detected at the pure array of TTAGGG repeats at DR_L-T2 (location shown in Fig. 5B) with the largest number of repeats in the HHV-6B Z29 reference genome and ciHHV-6B in HGDP00813 from China (Fig. 5A, Table 3). Notably, copy number variation observed at R0 (location shown in Fig. 1C) correlates reasonably well with the groups of ciHHV-6B genomes identified the phylogenetic network (Fig 5A; Table 3; Fig. 3).

Similar analysis of repeat regions in the ciHHV-6A genomes was conducted (Table 3). The data suggest that ciHHV-6A genomes have fewer TTAGGG repeats at DR_L-T2 than in the HHV-6A reference genomes. This variation could have been present in HHV-6A strains prior to integration or deletion mutations that reduce the length of the DR_L-T2 array may have been favoured after integration (12).

To explore variation within the T1 array of degenerate telomere-like repeats in ciHHV-6B genomes, we amplified the DR_R-T1 region by using the U100Fw2 and DR1R primers, and investigated the interspersion patterns of TTAGGG and degenerate repeats at the distal end of DR_R-T1 (near U100, Fig. 5B) by using modified TVR-PCR (36, 37, 42). Comparison of the TTAGGG interspersion patterns between the samples showed that the ciHHV-6B genomes clustered into groups that share similar TVR maps in DR_R-T1 (Fig. 5C).

346 Furthermore, these interspersion patterns differed between the groups and the singleton
347 ciHHV-6B genomes identified in the phylogenetic analyses. Variation around the $(CA)_n$
348 simple tandem repeat, located immediately adjacent to DR_L-T1 (location shown in Fig. 5B),
349 also showed clustering into groups that correlate with the ciHHV-6B phylogenetic analyses
350 (Fig 5D, Table 3, Fig. 3). Overall, the analyses of tandem repeat regions in the ciHHV-6B
351 genomes are consistent with the phylogenetic analyses.

352 **Ancestry of ciHHV-6B carriers in group 3.** The repeat copy number variation observed
353 within and among groups may have arisen before or after telomeric integration of the viral
354 genome. To investigate further how many different integration events may have occurred
355 among the ciHHV-6B carriers, we isolated and sequenced fragments containing the junction
356 between the human chromosome and the ciHHV-6B genome, in addition to using the
357 cytogenetic locations published previously for some samples (Table 2; (16)). The junction
358 fragments were isolated by a trial-and-error approach, using PCR between a primer mapping
359 in DR8 in DR_R and a variety of primers known to anneal to different subtelomeric sequences
360 (Fig. 6A), including primers that anneal to the subterminal region of some but not all copies
361 of chromosome 17p (17p311 (43) and subT17-539 (12)). There was insufficient DNA for
362 analysis from the sequenced ORCA1340 (singleton) or the ORCA1622 and ORCA3835
363 (group 3) samples (Fig. 3B). However, analysis of DR_R-T1 and the other repeats showed that
364 the 42 ciHHV-6B carriers from Orkney fall into two groups, that share the same length at
365 DR_R-T1 with either ORCA1340 or with ORCA1622 and ORCA3835 (Table 3). For junction
366 fragment analysis, we selected ORCA1006 as a substitute for ORCA1340, since it shares the
367 same DR_R-T1 length. Similarly, ORCA1043, ORCA2119 and ORCA1263 were used as
368 substitutes for ORCA1622 and ORCA3835, since they share a different DR_R-TI length. Using
369 the chromosome 17p primers, junction fragments were generated from all of the group 3
370 ciHHV-6B samples and from 1-ciHHV-6B (a singleton in the phylogenetic network, Fig. 3).

371 Using these primers, PCR products were not amplified from other ciHHV-6B samples in this
372 study. The sequences of seven junction fragments from group 3 ciHHV-6B genomes
373 (including NWA008 (44), which is another ciHHV-6B carrier having a viral genome that
374 belongs to group 3 (data not shown)) were similar to each other but different from the
375 fragment in sample 1-ciHHV-6B (Fig. 6B). These data indicate the existence of at least two
376 independent integration events into different alleles of the chromosome 17p telomere, or
377 possibly into telomeres of different chromosomes that share similar subterminal sequences
378 (45).

379 Comparison of the junction fragments from group 3 ciHHV-6B samples shows
380 remarkably similar TTAGGG and degenerate repeat interspersion patterns (Fig. 6B). The
381 differences among the interspersion patterns are consistent with small gains or losses that may
382 have arisen from replication errors in the germline, after integration of the viral genome (36).
383 Therefore, it is most likely that the ciHHV-6B status of group 3 individuals arose from a
384 single ancestral integration event. Using the levels of nucleotide substitution between the
385 group 3 ciHHV-6B genomes, the time to the most recent common ancestor (TMRCA) was
386 estimated as 24,538 ±10,625 years ago (Table 4). This estimate is based on the assumption
387 that, once integrated, the ciHHV-6B genome mutates at the same average rate as the human
388 genome as a whole. However, deviation from this rate would result in an under- or over-
389 estimation of the TMRCA.

390 **Genetic intactness of ciHHV-6 genomes.** The evidence for an ancient origin of some,
391 probably most, of the ciHHV-6B genomes analysed, and for post-integration mutations in
392 repeat regions, raised the question of whether these genomes contain an intact set of viral
393 genes or whether they have been rendered non-functional by mutation. To explore the
394 consequence of sequence variation among the ciHHV6B genomes, the amino acid sequences
395 predicted from all genes in the ciHHV-6B genomes were aligned, and the cumulative

396 frequencies of independent synonymous and non-synonymous substitutions were determined
397 (Fig. 7A). The ratio of synonymous:non-synonymous substitutions varies among genes. The
398 great majority of non-synonymous changes (amounting to 34% of the total) result in single
399 amino acid substitutions, but one substitution in the U20 stop codon of HGDP00092 is
400 predicted to extend the coding region by eight codons. Only one substitution, which creates
401 an in-frame stop codon in U14 of 1-ciHHV-6B, is predicted to terminate a coding region
402 prematurely. Two of the seven ciHHV-6A genomes also have in-frame stop codons, one in
403 U79 of GLA_15137 and the other in U83 genes of GLA_4298 (data not shown).

404 The 21 inherited ciHHV-6B genomes are likely to include mutations that arose before
405 integration and represent variation among the parental non-integrated HHV-6B strains as well
406 as mutations that arose after integration. To explore the latter, five group 3 ciHHV-6B
407 genomes were compared (Fig. 7B). Among the ten substitutions identified, three were in non-
408 coding regions, one was a synonymous mutation in U77, and six were non-synonymous
409 mutations. From these limited data, it seems likely that the accumulation of mutations after
410 integration has been random in these ciHHV-6B genomes.

411 **DISCUSSION**

412 In this study, we used comparative analyses to explore diversity among ciHHV-6
413 genomes in order to understand the factors that influence the population frequencies of
414 ciHHV-6 and to determine whether the integrated genomes appear to retain the capacity for
415 full functionality as a virus. We have found that the ciHHV-6B genomes are more similar to
416 each another than to the two available HHV-6B reference genomes from Japan and
417 D.R.Congo (Figs 2, 3, 4 ; Supplementary Fig. S1*)*. This is particularly noticeable among the
418 19 ciHHV-6B genomes from individuals with European ancestry, which are more similar to
419 each other than they are to the ciHHV-6B genomes in HGDP00092 from Pakistan and

HGDP00813 from China. This pointer towards a relationship between the integrated HHV-6B strain and geographical distribution warrants further investigation, if the association between carrier status and potential disease risk is to be understood fully (21, 46). The smaller group of seven ciHHV-6A genomes show higher levels of divergence from the three available HHV-6A reference genomes from the USA, Uganda and the Gambia, and as reported previously (40). However, in making these observations, the possibility of sample bias should be considered, both in the geographic distribution of ciHHV-6 genomes analysed and, in particular, in the small number of non-integrated HHV-6A and HHV-6B genomes that are available for comparative analysis.

The isolation of chromosome junction fragments from eight ciHHV-6B samples (seven group 3 samples and 1-ciHHV-6B) by using primers from chromosome 17p subterminal sequences (43) suggests integration in alleles of the 17p telomere. Given the variable nature of human subterminal regions (45), the chromosome locations should be confirmed using a different approach. Nevertheless, comparison of the TTAGGG and degenerate repeat interspersion patterns at the chromosome-ciHHV-6B junction can be used to deduce relationships (42, 47) and, combined with the phylogenetic analyses, show that the individuals carrying a group 3 ciHHV-6B genome share an ancient ancestor. Group 3 includes individuals from Sardinia, England, Wales and Orkney, with greater divergence between the ciHHV-6B genomes in the two individuals from Sardinia (HGDP1065 and HGDP1077) than between the individual from Derby, England (DER512) and the Sardinian (HGDP1065) (Figs. 3, 5, 6 and Tables 2, 3). Moreover there is no evidence of a close family relationship between the two individuals from Sardinia. Overall, the data are consistent with the group 3 ciHHV-6B carriers being descendants of a common ancestor who existed approximately 24,500 years ago, similar to the date of the last glacial maximum and probably predating the colonization of Sardinia and Orkney.

445 The population screen of Orkney identified 42 ciHHV-6B carriers (frequency 1.9%,
446 Table 1*)* and no ciHHV-6A carriers, which also suggests a founder effect. However, the
447 Orkney ciHHV-6B samples can be divided into two groups, based on the length of DR_R-T1,
448 the ciHHV-6B phylogenetic analyses and the different integration sites. Therefore, it is likely
449 that the ciHHV-6B carriers in Orkney are the descendants of two different ciHHV-6B
450 ancestors, who may have migrated to Orkney independently. This is consistent with the fine
451 resolution genetic structure of the Orkney population and the history of Orkney, which
452 includes recent admixture from Norway (Norse-Vikings) (44).

453 Given the evidence that extant ciHHV-6B carriers in group 3 are descendants of a
454 single ancient founder with a germline integration, it is plausible that other clusters in the
455 phylogenetic tree have a similar history. For example the three individuals in group 2 may all
456 carry a ciHHV-6B integrated in a chromosome 11p telomere. Further verification is required
457 to support this speculation, and this will be valuable when assessing disease risk associated
458 with ciHHV-6 integrations in different telomeres.

459 There is good evidence that ciHHV-6 genomes can reactivate in some settings, for
460 example when the immune system is compromised (19, 20). However, it is not known what
461 proportion of ciHHV-6 genomes may retain the capacity to reactivate. We investigated this
462 question from various angles. We presented evidence that some ciHHV-6 genomes are
463 ancient and therefore could have accumulated inactivating mutations while in the human
464 genome. Most of the tandem repeats analysed in ciHHV-6B genomes showed minor
465 variations in repeat copy numbers (Fig. 5 and Table 3*)*. However, the function of these
466 regions is unclear, and, as copy number variation exits among the reference genomes, it seems
467 unlikely that the level of variation detected unduly influences the potential functionality of the
468 integrated viral genomes. In the protein-coding regions of ciHHV-6B genomes, 34% of
469 substitutions are non-synonymous and are predicted to cause amino acid substitutions (Fig.

7). A single potentially inactivating mutation was detected as an in-frame stop codon in gene U14 in 1-ciHHV-6B. Since this gene encodes a tegument protein that is essential for the production of viral particles and can induce cell cycle arrest at the G2/M phase (48), it seems unlikely that this integrated copy of ciHHV-6B would be able to reactivate. However, the other viral genes may be expressed in this ciHHV-6B genome and the presence of the viral genome may also affect telomere function. The stop codon in gene U20 in the individual from Pakistan (HGDP00092) is mutated, and this is predicted to extend the U20 protein by eight amino acid residues. U20 is part of a cluster of genes (U20-U24) that are specific to HHV-6A, HHV-6B and their relative human betaherpesvirus 7, and likely plays a role in suppressing an apoptotic response by the infected host cell (49, 50). Further experimental analysis will be required to determine whether the modest extension affects the function of the U20 protein. Among the seven ciHHV-6A genomes, two contain novel in-frame stop codons. One of these is located in U83 in GLA_4298. The other is present in U79 in GLA_15137, but this inactivating mutation is absent from the closely related ciHHV-6A genome in 7A-17p13.3 (Fig. 3C and D).

In summary, we have shown that most ciHHV-6A and ciHHV-6B genomes contain an intact set of genes and therefore may have the potential to be fully functional. This observation needs to be taken into consideration when assessing whether ciHHV-6 carrier status is associated with disease risk and in understanding the underlying mechanisms of such associations (e.g. whether viral reactivation is involved). Among the individuals of European descent, we found strong evidence for the ancient common ancestry of some of the integrated viral genomes. The close similarity between ciHHV-6B genomes in the Europeans and the evidence of multiple different integration events by similar strains also indicate that we have effectively sequenced the ancient, non-integrated strains of HHV-6B that existed in European populations in prehistoric times. Based on these observations, it is possible that other

populations, for example in China, South Asia and Africa, may show similar founder effects among ciHHV-6 carriers but from different ancient strains (51). Our limited knowledge of non-integrated HHV-6A and HHV-6B strains is based mostly on strains derived from Africa and Japan. There is now a real need to sequence non-integrated strains from other populations, including those in Europe, so that the relationship between non-integrated HHV-6 and ciHHV-6 can be fully understood. A major challenge will be to determine whether germline integration continues to occur *de novo* today, and, if so, at what rate and by which viral strains.

ACKNOWLEDGMENTS

We thank most sincerely Mark Jobling, Michael Wood and Ryan Mate (University of Leicester) for their help with data analysis. We also thank Martin Dyer (University of Leicester), Bruce Winney (University of Oxford), James F. Wilson (University of Edinburgh) and Duncan A. Clark (Department of Virology, Barts Health NHS Trust) for samples from the various populations screened. Author contributions: EZ, AJB, GSW, NMS, RN, IA-C, VEC, and YH conducted various aspects of the experimental work; AJD, EZ, GSW, NMS, CDV, and CB conducted the bioinformatic and other analyses; DJP is a member of the Executive Committee of Generation Scotland and, with AJB and RFJ, screened the large GS: SFHS cohort to identify ciHHV-6 carriers used in this study; NJR was responsible for the project design. The paper was written by EZ and NJR with significant input from AJD and RFJ.

FUNDING

This work was supported by the UK Medical Research Council [G0901657 to N.J.R., MC_UU_12014/3 to A.J.D.] and the Wellcome Trust Institutional Strategic Support Fund [WT097828MF to N.J.R]. Generation Scotland receives core support from the Chief Scientist

519 Office of the Scottish Government Health Directorates [CZD/16/6] and the Scottish Funding
520 Council [HR03006].

521 **REFERENCES**

522 1. Holohan B, Wright WE, Shay JW. 2014. Cell biology of disease: Telomeropathies: an
523 emerging spectrum disorder. J Cell Biol 205:289-99.
524 2. Reddel RR. 2010. Senescence: an antiviral defense that is tumor suppressive? Carcinogenesis
525 31:19-26.
526 3. Ablashi D, Agut H, Alvarez-Lafuente R, Clark DA, Dewhurst S, DiLuca D, Flamand L,
527 Frenkel N, Gallo R, Gompels UA, Hollsberg P, Jacobson S, Luppi M, Lusso P, Malnati M,
528 Medveczky P, Mori Y, Pellett PE, Pritchett JC, Yamanishi K, Yoshikawa T. 2014.
529 Classification of HHV-6A and HHV-6B as distinct viruses. Arch Virol 159:863-70.
530 4. de Lange T. 2005. Shelterin: the protein complex that shapes and safeguards human
531 telomeres. Genes Dev 19:2100-10.
532 5. Sfeir A, de Lange T. 2012. Removal of shelterin reveals the telomere end-protection problem.
533 Science 336:593-7.
534 6. Arnoult N, Karlseder J. 2015. Complex interactions between the DNA-damage response and
535 mammalian telomeres. Nat Struct Mol Biol 22:859-66.
536 7. Lindquester GJ, Pellett PE. 1991. Properties of the human herpesvirus 6 strain Z29 genome: G
537 + C content, length, and presence of variable-length directly repeated terminal sequence
538 elements. Virology 182:102-10.
539 8. Achour A, Malet I, Deback C, Bonnafous P, Boutolleau D, Gautheret-Dejean A, Agut H.
540 2009. Length variability of telomeric repeat sequences of human herpesvirus 6 DNA. J Virol
541 Methods 159:127-30.
542 9. Dominguez G, Dambaugh TR, Stamey FR, Dewhurst S, Inoue N, Pellett PE. 1999. Human
543 herpesvirus 6B genome sequence: coding content and comparison with human herpesvirus
544 6A. J Virol 73:8040-52.
545 10. De Bolle L, Naesens L, De Clercq E. 2005. Update on human herpesvirus 6 biology, clinical
546 features, and therapy. Clin Microbiol Rev 18:217-45.
547 11. Arbuckle JH, Medveczky MM, Luka J, Hadley SH, Luegmayr A, Ablashi D, Lund TC, Tolar
548 J, De Meirleir K, Montoya JG, Komaroff AL, Ambros PF, Medveczky PG. 2010. The latent
549 human herpesvirus-6A genome specifically integrates in telomeres of human chromosomes in
550 vivo and in vitro. Proc Natl Acad Sci U S A 107:5563-8.
551 12. Huang Y, Hidalgo-Bravo A, Zhang E, Cotton VE, Mendez-Bermudez A, Wig G, Medina-
552 Calzada Z, Neumann R, Jeffreys AJ, Winney B, Wilson JF, Clark DA, Dyer MJ, Royle NJ.
553 2014. Human telomeres that carry an integrated copy of human herpesvirus 6 are often short

and unstable, facilitating release of the viral genome from the chromosome. Nucleic Acids Res 42:315-27.

13. Daibata M, Taguchi T, Nemoto Y, Taguchi H, Miyoshi I. 1999. Inheritance of chromosomally integrated human herpesvirus 6 DNA. Blood 94:1545-9.

14. Morris C, Luppi M, McDonald M, Barozzi P, Torelli G. 1999. Fine mapping of an apparently targeted latent human herpesvirus type 6 integration site in chromosome band 17p13.3. J Med Virol 58:69-75.

15. Tanaka-Taya K, Sashihara J, Kurahashi H, Amo K, Miyagawa H, Kondo K, Okada S, Yamanishi K. 2004. Human herpesvirus 6 (HHV-6) is transmitted from parent to child in an integrated form and characterization of cases with chromosomally integrated HHV-6 DNA. J Med Virol 73:465-73.

16. Nacheva EP, Ward KN, Brazma D, Virgili A, Howard J, Leong HN, Clark DA. 2008. Human herpesvirus 6 integrates within telomeric regions as evidenced by five different chromosomal sites. J Med Virol 80:1952-8.

17. Prusty BK, Krohne G, Rudel T. 2013. Reactivation of chromosomally integrated human herpesvirus-6 by telomeric circle formation. PLoS Genet 9:e1004033.

18. Zhang E, Cotton VE, Hidalgo-Bravo A, Huang Y, J. Bell A, F. Jarrett R, Wilkie GS, Davison AJ, P. Nacheva E, Siebert R, Majid A, Kelpanides I, Jayne S, Dyer MJ, Royle NJ. 2016. HHV-8-unrelated primary effusion-like lymphoma associated with clonal loss of inherited chromosomally-integrated human herpesvirus-6A from the telomere of chromosome 19q. Scientific Reports 6:22730.

19. Endo A, Watanabe K, Ohye T, Suzuki K, Matsubara T, Shimizu N, Kurahashi H, Yoshikawa T, Katano H, Inoue N, Imai K, Takagi M, Morio T, Mizutani S. 2014. Molecular and virological evidence of viral activation from chromosomally integrated human herpesvirus 6A in a patient with X-linked severe combined immunodeficiency. Clin Infect Dis 59:545-8.

20. Gravel A, Hall CB, Flamand L. 2013. Sequence analysis of transplacentally acquired human herpesvirus 6 DNA is consistent with transmission of a chromosomally integrated reactivated virus. J Infect Dis 207:1585-9.

21. Gravel A, Dubuc I, Morissette G, Sedlak RH, Jerome KR, Flamand L. 2015. Inherited chromosomally integrated human herpesvirus 6 as a predisposing risk factor for the development of angina pectoris. Proc Natl Acad Sci U S A 112:8058-63.

22. Bell AJ, Gallagher A, Mottram T, Lake A, Kane EV, Lightfoot T, Roman E, Jarrett RF. 2014. Germ-line transmitted, chromosomally integrated HHV-6 and classical Hodgkin lymphoma. PLoS One 9:e112642.

23. Gompels UA, Nicholas J, Lawrence G, Jones M, Thomson BJ, Martin ME, Efstathiou S, Craxton M, Macaulay HA. 1995. The DNA sequence of human herpesvirus-6: structure, coding content, and genome evolution. Virology 209:29-51.

24. Leong HN, Tuke PW, Tedder RS, Khanom AB, Eglin RP, Atkinson CE, Ward KN, Griffiths PD, Clark DA. 2007. The prevalence of chromosomally integrated human herpesvirus 6 genomes in the blood of UK blood donors. J Med Virol 79:45-51.

25. Isegawa Y, Mukai T, Nakano K, Kagawa M, Chen J, Mori Y, Sunagawa T, Kawanishi K, Sashihara J, Hata A, Zou P, Kosuge H, Yamanishi K. 1999. Comparison of the complete DNA sequences of human herpesvirus 6 variants A and B. J Virol 73:8053-63.

26. Bankevich A, Nurk S, Antipov D, Gurevich AA, Dvorkin M, Kulikov AS, Lesin VM, Nikolenko SI, Pham S, Prjibelski AD, Pyshkin AV, Sirotkin AV, Vyahhi N, Tesler G, Alekseyev MA, Pevzner PA. 2012. SPAdes: a new genome assembly algorithm and its applications to single-cell sequencing. J Comput Biol 19:455-77.

27. Assefa S, Keane TM, Otto TD, Newbold C, Berriman M. 2009. ABACAS: algorithm-based automatic contiguation of assembled sequences. Bioinformatics 25:1968-1969.

28. Boetzer M, Pirovano W. 2012. Toward almost closed genomes with GapFiller. Genome Biology 13.

29. Salahuddin SZ, Ablashi DV, Markham PD, Josephs SF, Sturzenegger S, Kaplan M, Halligan G, Biberfeld P, Wong-Staal F, Kramarsky B, Gallo R. 1986. Isolation of a new virus, HBLV, in patients with lymphoproliferative disorders. Science 234:596-601.

30. Gravel A, Ablashi D, Flamand L. 2013. Complete Genome Sequence of Early Passaged Human Herpesvirus 6A (GS Strain) Isolated from North America. Genome Announc 1.

31. Tweedy J, Spyrou MA, Donaldson CD, Depledge D, Breuer J, Gompels UA. 2015. Complete Genome Sequence of the Human Herpesvirus 6A Strain AJ from Africa Resembles Strain GS from North America. Genome Announc 3.

32. Staden R, Beal KF, Bonfield JK. 2000. The Staden package, 1998. Methods Mol Biol 132:115-30.

33. Tamura K, Stecher G, Peterson D, Filipski A, Kumar S. 2013. MEGA6: Molecular Evolutionary Genetics Analysis version 6.0. Mol Biol Evol 30:2725-9.

34. Scally A, Durbin R. 2012. Revising the human mutation rate: implications for understanding human evolution. Nat Rev Genet 13:745-53.

35. Baird DM, Rowson J, Wynford-Thomas D, Kipling D. 2003. Extensive allelic variation and ultrashort telomeres in senescent human cells. Nat Genet 33:203-7.

36. Baird DM, Jeffreys AJ, Royle NJ. 1995. Mechanisms underlying telomere repeat turnover, revealed by hypervariable variant repeat distribution patterns in the human Xp/Yp telomere. EMBO Journal 14:5433-5443.

37. Varley H, Pickett HA, Foxon JL, Reddel RR, Royle NJ. 2002. Molecular characterization of inter-telomere and intra-telomere mutations in human ALT cells. Nat Genet 30:301-5.

38. Moustafa A, Xie C, Kirkness E, Biggs W, Wong E, Turpaz Y, Bloom K, Delwart E, Nelson KE, Venter JC, Telenti A. 2017. The blood DNA virome in 8,000 humans. PLoS Pathog 13:e1006292.

39. Downing RG, Sewankambo N, Serwadda D, Honess R, Crawford D, Jarrett R, Griffin BE. 1987. Isolation of human lymphotropic herpesviruses from Uganda. Lancet 2:390.

40. Tweedy J, Spyrou MA, Pearson M, Lassner D, Kuhl U, Gompels UA. 2016. Complete Genome Sequence of Germline Chromosomally Integrated Human Herpesvirus 6A and Analyses Integration Sites Define a New Human Endogenous Virus with Potential to Reactivate as an Emerging Infection. Viruses 8.

41. Chakraborty R, Kimmel M, Stivers DN, Davison LJ, Deka R. 1997. Relative mutation rates at di-, tri-, and tetranucleotide microsatellite loci. Proc Natl Acad Sci U S A 94:1041-6.

42. Mendez-Bermudez A, Hills M, Pickett HA, Phan AT, Mergny JL, Riou JF, Royle NJ. 2009. Human telomeres that contain (CTAGGG)n repeats show replication dependent instability in somatic cells and the male germline. Nucleic Acids Res 37:6225 - 6238.

43. Britt-Compton B, Rowson J, Locke M, Mackenzie I, Kipling D, Baird DM. 2006. Structural stability and chromosome-specific telomere length is governed by cis-acting determinants in humans. Hum Mol Genet 15:725-33.

44. Leslie S, Winney B, Hellenthal G, Davison D, Boumertit A, Day T, Hutnik K, Royrvik EC, Cunliffe B, Wellcome Trust Case Control C, International Multiple Sclerosis Genetics C, Lawson DJ, Falush D, Freeman C, Pirinen M, Myers S, Robinson M, Donnelly P, Bodmer W. 2015. The fine-scale genetic structure of the British population. Nature 519:309-14.

45. Riethman H. 2008. Human telomere structure and biology. Annu Rev Genomics Hum Genet 9:1-19.

46. Pinto EM, Chen X, Easton J, Finkelstein D, Liu Z, Pounds S, Rodriguez-Galindo C, Lund TC, Mardis ER, Wilson RK, Boggs K, Yergeau D, Cheng J, Mulder HL, Manne J, Jenkins J, Mastellaro MJ, Figueiredo BC, Dyer MA, Pappo A, Zhang J, Downing JR, Ribeiro RC, Zambetti GP. 2015. Genomic landscape of paediatric adrenocortical tumours. Nat Commun 6:6302.

47. Mendez-Bermudez A, Hidalgo-Bravo A, Cotton VE, Gravani A, Jeyapalan JN, Royle NJ. 2012. The roles of WRN and BLM RecQ helicases in the Alternative Lengthening of Telomeres. Nucleic Acids Res 40:10809-20.

48. Mori J, Kawabata A, Tang H, Tadagaki K, Mizuguchi H, Kuroda K, Mori Y. 2015. Human Herpesvirus-6 U14 Induces Cell-Cycle Arrest in G2/M Phase by Associating with a Cellular Protein, EDD. PLoS One 10:e0137420.

49. Kofod-Olsen E, Ross-Hansen K, Schleimann MH, Jensen DK, Moller JM, Bundgaard B, Mikkelsen JG, Hollsberg P. 2012. U20 is responsible for human herpesvirus 6B inhibition of tumor necrosis factor receptor-dependent signaling and apoptosis. J Virol 86:11483-92.

663 50. Jasirwan C, Tang H, Kawabata A, Mori Y. 2015. The human herpesvirus 6 U21-U24 gene
664 cluster is dispensable for virus growth. Microbiol Immunol 59:48-53.
665 51. Kawamura Y, Ohye T, Miura H, Ihira M, Kato Y, Kurahashi H, Yoshikawa T. 2017. Analysis
666 of the origin of inherited chromosomally integrated human herpesvirus 6 in the Japanese
667 population. J Gen Virol doi:10.1099/jgv.0.000834.

668

669

670 Table 1. Summary of populations screened for ciHHV-6

	Region	Samples	Total ciHHV-6	ciHHV-6A	ciHHV-6B
Africa	Sub-Saharan Africa	105	0	0	0
	North Africa	29	0	0	0
Europe	North European Extraction (CEPH)	136	2	0	2
	British	518	7	1	6
	Orkney	2194	42 (1.9%)	0	42
	Italy (including Sardinia)	49	2	0	2
	France	52	0	0	0
	Russia	42	0	0	0
Middle East	Israel	134	2	2	0
South/Central Asia	Pakistan	192	1	0	1
	Uygur (China)	10	0	0	0
East Asia	China	213	1	0	1
	Japan	74	1	1	0
	Others (Siberia & Cambodia)	35	0	0	0
Oceania	Bougainville	17	0	0	0
	New Guinea	11	0	0	0
America	South America	29	0	0	0
	Mexico	35	0	0	0
TOTAL		3875	58	4	54

671 [a] In addition AJB, RFJ and colleagues have screened the Generation Scotland: Scottish Family Health
672 Study cohort for ciHHV-6 (manuscript in preparation).

673

674

675 Table 2. Samples from individuals with ciHHV-6 selected for viral genome sequencing.

Sample	Acc. No	ciHHV-6	Integration Site [a]	Population or Country
LEI-1501 [b]	KT355575	A	19q	Leicester area (England)
HAPMAP NA18999	KY316047	A	-	Japan
3A-10q26.3 [c]	KY316049	A	10q26.3 & junction isolated by PCR	South-East England
GLA_4298 [d]	KY316056	A	-	Newcastle (England)
GLA_15137 [e]	KY316055	A	-	Scotland
GLA_ 25506 [e]	KY316054	A	-	Scotland
7A-17p13.3 [c]	KY316048	A	17p13.3	South-East England
HGDP00092	KY316037	B	-	Balochi (Pakistan)
HGDP00813	KY316036	B	-	Han (China)
HGDP01065	KY316035	B	Junction isolated by PCR	Sardinia (Italy)
HGDP01077	KY316034	B	Junction isolated by PCR	Sardinia (Italy)
HAPMAP NA07022 (CEPH 1340.11)	KY316039	B	-	Utah Mormon (North European)
HAPMAP NA10863 (CEPH-1375.02)	KY316038	B	-	Utah Mormon (North European)
4B-11p15.5 [c]	KY316044	B	11p15.5	Southern East England
BAN519 [f]	KY316043	B	-	Banff (Scotland)
COR264 [f]	KY316042	B	-	Cornwall (England)
CUM082 [f]	KY316041	B	-	Cumbria (England)
DER512 [f]	KY316040	B	Junction isolated by PCR	Derbyshire (England)
2B-9q34.3 [c]	KY316045	B	9q34.3	South-East England
1-ciHHV-6B [c]	KY316046	B	Junction isolated by PCR	South-East England
LEI-ALD	KY316033	B	-	Leicester area (England)
ORCA1622	KY316031	B	-	Orkney
ORCA1340	KY316032	B	-	Orkney
ORCA3835	KY316030	B	-	Orkney
GLA_3986 [d]	KY316053	B	-	Newcastle (England)
GLA_29221 [e]	KY316052	B	-	Scotland
GLA_34108 [e]	KY316051	B	-	Scotland
GLA_35629 [e]	KY316050	B	-	Scotland

[a] Determined by FISH or amplification of chromosme-ciHHV-6 junctions by PCR; [b] LEI-1501 described in (18); [c] ciHHV-6 carriers describe in (16); [d] ciHHV-6 carriers previously described in (22); [e] ciHHV-6 carriers identified in the GS: SFHS; [f] Samples from the Population of British Isles study (44).

676

677 Table 3. Variation in tandem repeat regions among ciHHV-6.

Tandem repeat regions in HHV-6B

Name	T1	STR $(CA)_n$	R-DR [a]	T2	R0 [a]	R1	R2A [a]	R2B	R3	R4 [a]
Location		adjacent to DR-T1	DR	DR	U1	U86	U86-U89	U86-U89	U91-U94	After U100
Length (bp)	6	2	15	6	~15	12	79	12 - 15	~104	64
Unit		CA	NI [b]	(TTAGGG)	NI	NI	NI	NI	NI	NI
HST [c]	-	12	6	26	17	51	4	6	-	6
Z29 [c]	-	1	4	77	13	53	4	8	-	4
HAPMAP NA10863	-	20	5	28	16	44	4	7	-	4
2B-9q34.3	-	20	5	26	19	44	4	7	-	4
CUM082	-	19	5	27	19	45	4	7	-	4
BAN519	-	19	5	28	16	44	4	7	-	4
GLA_3986	-	20	5	-	19	44	4	7	-	2
GLA_29221	-	19	5	-	19	45	4	7	-	4
GLA_34108	-	19	5	-	19	43	4	7	-	4
GLA_35629	-	-	5	-	19	45	4	7	-	4
HAPMAP NA07022	-	11	5	29	10	46	4	6	-	4
4B-11p15.5	-	11	5	26	10	47	4	6	-	4
LEI-ALD	-	11	5	25	10	47	4	6	-	4
HGDP01065	-	10	5	15	16	44	4	7	-	4
HGDP01077	-	10	5	19	16	43	4	7	-	4
DER512	-	10	5	21	16	43	4	7	-	4
ORCA1622	-	-	5	-	16	43	4	7	-	3
ORCA3835	-	-	5	-	16	43	4	7	-	3
ORCA1340	-	-	-	-	16	48	4	6	-	4
1-ciHHV-6B	-	12	5	16	16	43	4	6	-	4
COR264	-	12	9	28	19	44	4	7	-	2
HGDP00813	-	20	3	53	12	52	4	7	-	4
HGDP00092	-	1	2	19	17	55	4	11	-	3

Tandem repeat regions in HHV-6A

	T1	T2	R5 [d]	R1	R2	R3
Location		DR	U41 - U42	U86	U86 -U89	U91 -U94
Length (bp)	6	6	~191	~12	12-18	104-105
		(TTAGGG)	NI	NI	NI	NI
AJ [c]	-	51	1.7	52	43	8
U1102 [c]	-	59	1.7	52	102	29
GS1/2 [c]	-	51	1.7	52	78	8
LEI-1501	-	14	2.7	-	-	-
GLA_25506	-	-	2.7	32	-	-
GLA_4298	-	-	3.7	53	-	-
HAPMAP NA18999	-	13	1.7	-	-	-
3A-10q26.3	-	9	1.7	58	-	-
GLA_15137	-	-	1.7	55	-	-
7A-17p13.3	-	-	1.7	55	-	-

[a] Repeats specific to HHV-6B - the coordinates of R-DR and R4 in HHV-6B strain HST are 5400-5489 and 152603-152986 respectively; [b] NI, repeats not identical; [c] Reference genomes in bold; [d] Repeat specific to HHV-6A - the coordinates of R5 in HHV-6A strain U1102 are 68124-68450; the other repeats are described in (9) (25); hyphens, analysis not completed. The samples in the same box are in the same group in the phylogenetic networks.

678

679 Table 4. Estimate of TMRCA for ciHHV-6B genomes in group 3.

	Entire group 3 [a]	HGDP1065 & HGDP1077	HGDP1065 & DER512
TMRCA (y)	24,538	23,004	15,336
Standard deviation	10,625	13,281	10,844

[a] ORCA1622 and ORCA3835 are identical across non-repeat regions.

680

681

682 **Figure Captions**

683 **Figure 1.** Approach to sequencing ciHHV-6 genomes. (A) Diagram showing the
684 organisation of the HHV-6 genome following integration of a single full-length copy into a
685 telomere. Chromosome and centromere (Cen) are shown by blue lines and an oval. The
686 telomere repeats are shown by red arrows. The telomere, encompassing DR_L-T1, is shown by
687 a red dashed line. The junction between the chromosome and HHV-6 genome, encompassing
688 telomere repeats and DR_R-T2, is shown by a dashed blue line. DR_L and DR_R are shown as
689 blue boxes. *(*B) Distribution of numbered PCR amplicons across the HHV-6B genome and an
690 example gel of PCR products generated from 1-ciHHV-6B. (C) Sequence coverage for
691 individual ciHHV-6B genomes. Each ciHHV-6B genome is shown with a single DR (blue
692 box) that was covered by amplicons from DR_L and DR_R and with U (grey box). Gaps in the
693 coverage caused by loss of individual amplicons at the amplicon-pooling stage are shown in
694 white. Tandem repeat regions that were fully sequenced by either Illumina NGS or by the
695 Sanger method are shown in orange. Tandem repeat regions (e.g. T1 and R3 in HHV-6B) that
696 were too long to be sequenced fully are shown as hashed-brown boxes. (D) Distribution of
697 numbered PCR amplicons across the HHV-6A genome and an example gel of products
698 generated from HAPMAP NA18999. (E). Sequence coverage for each ciHHV-6A genomes,
699 using the same colour coding as in (C).

700

701 **Figure 2.** Frequency of nucleotide substitutions in ciHHV-6 genomes compared to reference
702 viral genomes. (A) Graphs showing the number of substitutions in 1 kb windows for each of
703 the 21 ciHHV-6B genomes in comparison with the HHV-6B strain HST (Japan) and Z29
704 (D.R.Congo) genomes (top and middle panels, respectively) and the ciHHV-6B genome from
705 HAPMAP NA10863 (bottom panel). The colour-coded key shows that ciHHV-6B genomes
706 from individuals with European ancestry are represented as light blue lines; ciHHV-6B in
707 HGDP00813 (China), red lines; ciHHV-6B in HGDP00092 (Pakistan), black lines. (B)
708 Graphs showing the number of substitutions in 1 kb windows for each of the 7 ciHHV-6A
709 genomes in comparison with the HHV-6A strain U1102 (Uganda), GS (USA) and AJ
710 (Gambia) genomes (top and two middle panels) and the ciHHV-6A genome in LEI-1501
711 (bottom panel). The colour-coded key distinguishes the ciHHV-6A genomes. The x-axes in
712 all the graphs show the HHV-6B and -6A genomes with a single DR (0-8kb) followed by U

(9-150kb) as shown in Figure 1C and 1E. Variation within the tandem repeat regions is not shown in these graphs.

Figure 3. Phylogenetic analysis of ciHHV-6 and reference non-integrated HHV-6 genomes. (A) Maximum likelihood phylogenetic tree of 21 ciHHV-6B genomes and two HHV-6B reference genomes (strains HST (Japan) and Z29 (D.R Congo)). A total of 130412 nucleotides were analysed, excluding repeat regions and missing amplicons. The scale bar represents 0.0005 substitutions per site. (B) Phylogenetic network generated from the dataset used in (A), but without the HST and Z29 genomes and the ciHHV-6B genomes from HGDP00813 (China) and HGDP00092 (Pakistan). The ciHHV-6B genomes from Europeans in groups 1, 2 and 3 are shown as blue, orange and green dots, respectively and the singletons are shown as grey dots. (C) Maximum likelihood phylogenetic tree of seven ciHHV-6A genomes and four HHV-6A reference genomes (strains U1102 (Uganda), AJ (Gambia), GS1 (USA) and GS2 (USA); GS1 and GS2 are two versions of strain GS). A total of 117900 nucleotides were analysed, excluding repeat regions and missing amplicons. The scale bar represents 0.002 substitutions per site. (D) Phylogenetic network generated from the dataset used in (C). The non-integrated HHV-6A reference genomes are shown as yellow dots. The closely related ciHHV-6A genomes are shown as pairs of red or blue dots and singletons as grey dots (including one from Japan). The scale bars in the networks (C and D) show the number of base substitutions for a given line length. The dots are scaled, the smallest dot representing a single individual.

Figure 4. Frequency of nucleotide substitutions in ciHHV-6 genes compared to those in reference viral genomes. (A) Graphs of substitution frequency in each gene are shown for the 21 ciHHV-6B genomes in comparison with HHV-6B strains HST (Japan) and Z29 (D.R.Congo) genomes (top and middle panels, respectively) and the ciHHV-6B genome in European HAPMAP NA10863 (bottom panel). The colour coding shown in the key matches that of the network in Figure 3B as follows: European Group 1, pale blue lines; European Group 2, orange lines; European Group 3, green lines; European singletons, grey lines; ciHHV-6B in HGDP00813 from China, red lines; and ciHHV-6B in HGDP00092 from Pakistan, black lines. (B) Graphs of substitution frequency in each gene for each of the 7 ciHHV-6A genomes in comparison with the HHV-6A strains U1102 (Uganda), GS (USA)

and AJ (Gambia) genomes (top and two middle panels) and the ciHHV-6A genome in European LEI-1501 (bottom panel). The colour-coded key matches that of the network in Figure 3D. The x-axes of all the graphs show a single copy of DR1 and DR6, followed by genes found in the U region.

Figure 5. Copy number variation in tandem repeat loci across the HHV-6B genome. (A) Graph of the number of repeat units at loci within the DR (R-DR and DR_L-T2) and U regions (R0, R1, R2A, R2B and R4). Comparisons can be made among the reference non-integrated HHV-6B strains, HST (Japan) and Z29 (D.R. Congo) and ciHHV-6B genomes. The sample order along the x-axis as follows: HST, Z29 (mauve highlight); European group 1 ciHHV-6B genomes (blue highlight); European group 2 ciHHV-6B genomes (orange highlight); European group 3 ciHHV-6B genomes (green highlight); European singleton ciHHV-6B genomes (no highlight); ciHHV-6B in HGDP00813 from China (red highlight); and ciHHV-6B in HGDP00092 from Pakistan (no highlight). (B) Diagram showing the location of the PCR amplicons used to analyse the repeat sequences shown in C and D. Black dashed line shows the amplicon generated by the U100Fw2 and DR1R primers that were used for TVR-PCR shown in (C). Red dashed line shows STELA products, generated from DR1R, that were used to analysis the $(CA)_n$ repeat shown in D. (C) Distribution of (TTAGGG) repeats at the distal end of DR_R-T1 (near U100) in ciHHV-6B genomes. If the repeat array comprises consecutive TTAGGG repeats, a ladder of bands with 6 base periodicity should be present and the migration distance between the rungs on the ladder should steadily decrease as the separation between the bands is reduced (near the top of the gel, towards DR1). The observed distance between the bands in each track varies between the samples. This shows that the repeat array is not pure $(TTAGGG)_n$ but includes intervening sequence, most likely degenerate telomere-like repeats. The pattern of repeats can be compared between the tracks to identify samples that share the same repeat distribution at this end of the DR_R-T1. The ciHHV-6B sample names are colour-coded in accordance with groupings identified in Figure 3: European group 1, blue; group 2, orange; group 3, green; European singletons, grey; ciHHV-6B in HGDP00813 from China, red; ciHHV-6B in HGDP00092 from Pakistan, black. (D) Variation in copy number of (CA) repeats and adjacent 5'- sequence, near the start of the ciHHV-6B DR_L-T1 region. Sample names colour-coded as described in (C).

Figure 6. Characterisation of ciHHV-6B integration sites. (A) Diagram showing the location of PCR amplicons used to characterise the chromosome-ciHHV-6B junctions. Red arrows represent TTAGGG and degenerate repeats. Blue arrows, primers used to amplify the chromosome-HHV-6 junction; blue dashed line, chromosome-junction amplicon used for sequence analysis. (B) Diagram showing the similarity of the TTAGGG (red squares) and degenerate repeat (coloured squares in key to right) interspersion patterns in the chromosome-HHV-6 junctions from individuals with group 3 ciHHV-6B genomes (DER512 to HGDP01065, Figure 3B). These interspersion patterns are distinct from that of the chromosome-junction fragment isolate from 1-ciHHV-6B (singleton in Figure 3B). The sequence to the left of the repeats is from the chromosome subtelomeric region and the sequence to the right is from the ciHHV-6B genome.

Figure 7. Consequences of nucleotide substitutions across the ciHHV-6 genome. (A) Comparison of synonymous (blue) and non-synonymous (orange) substitution frequencies in each ciHHV-6B gene among the 21 ciHHV-6B genomes (scaled to differences per 1000 amino acids). The green dot shows the novel in-frame stop codon in U14 of 1-ciHHV-6B. The pie chart shows the overall proportions of synonymous and non-synonymous substitutions across all genes. (B) Diagram showing the approximate location and consequence of nucleotide substitutions that are predicted to have arisen after integration in group 3 ciHHV-6B genomes. The horizontal line represents the HHV-6B genome; black dots, location of non-coding base substitutions; red dots, base substitutions within HHV-6B genes that are predicted to result in an amino acid substitutions (non-synonymous) shown by the text; pink dot, synonymous (T to C) substitution in DER512 that is not predicted to change the phenylalanine. HGDP01065, green text; HGDP01077, orange text; DER512 in blue and the identical sequences found in ORCA1622 and ORCA3835 in purple. The number of repeats in three regions (T2, R1 and R4) that vary among the group 3 genomes are also shown.

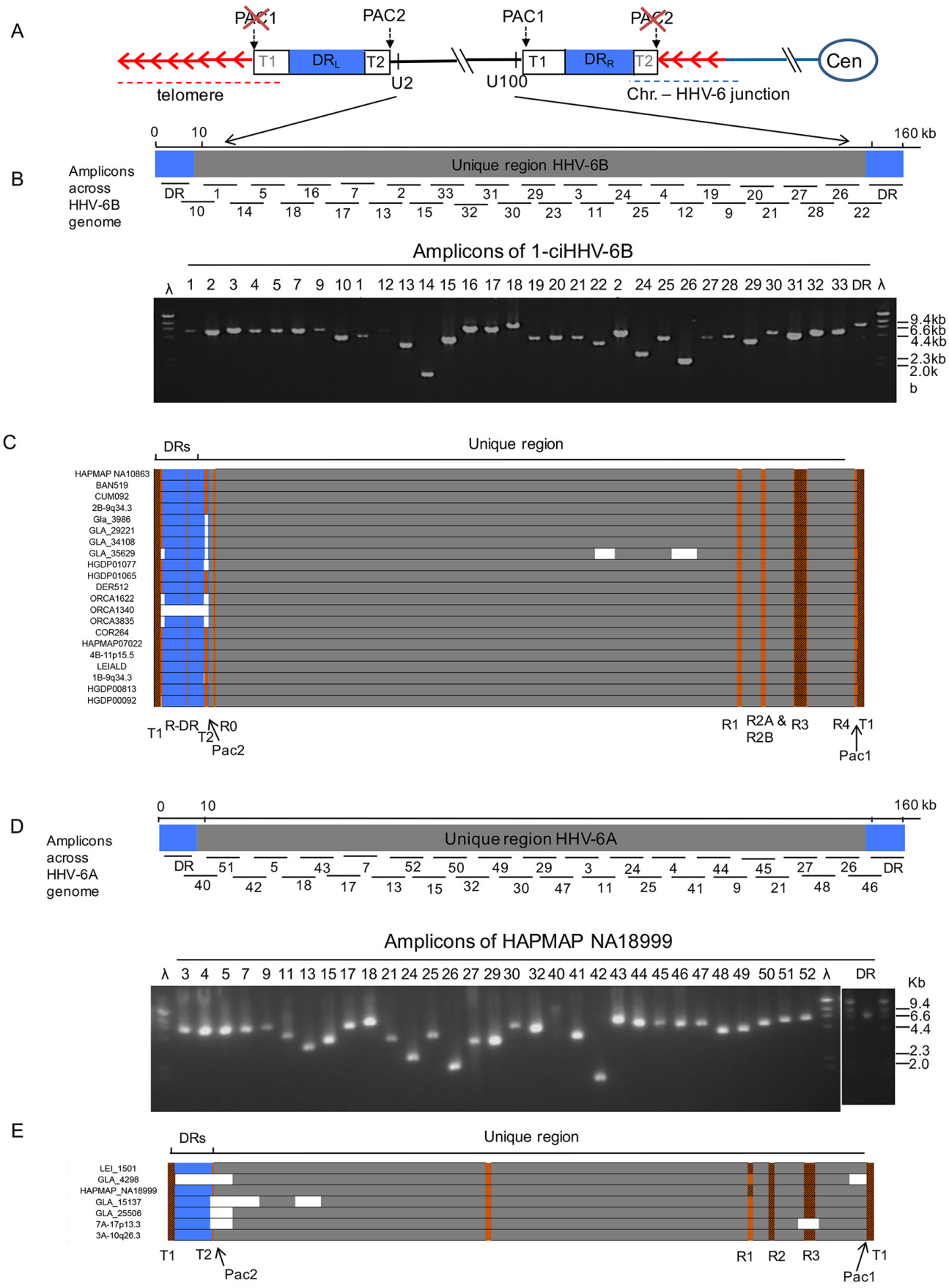

Journal of Virology

JVI

Journal of Virology

A

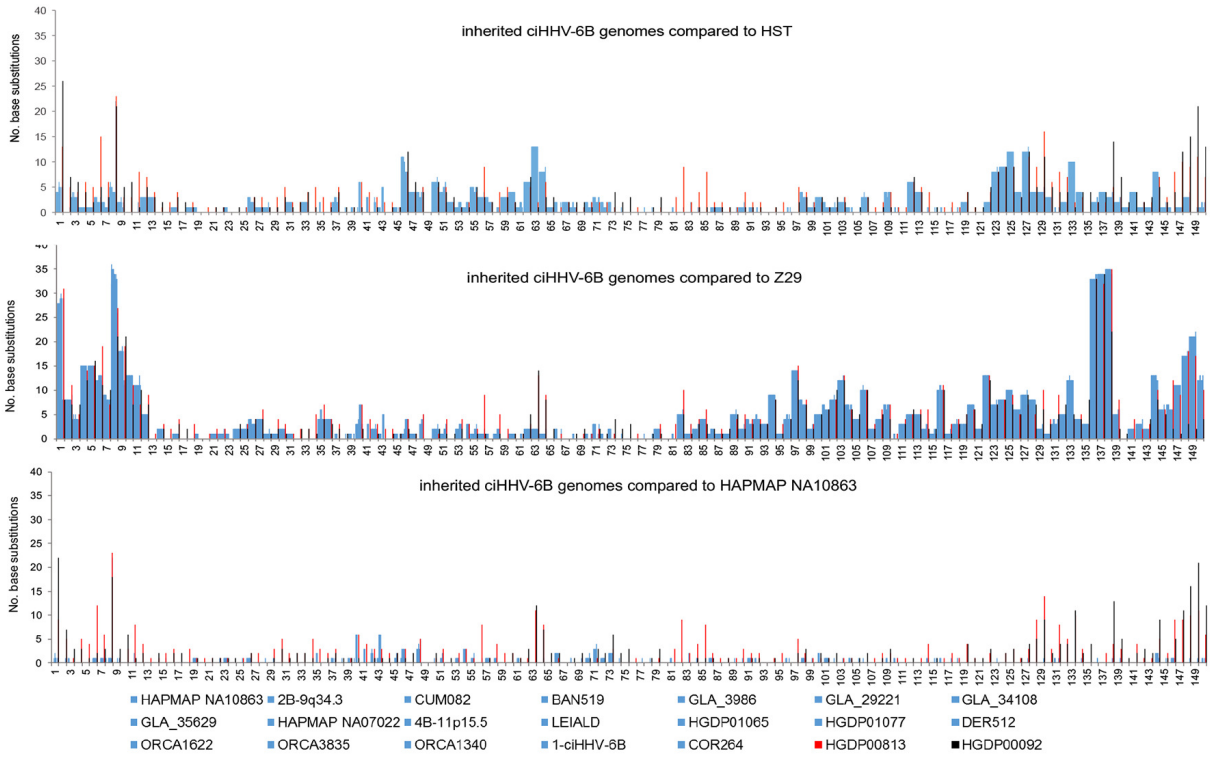

B